H, 2.50; H, 10.66. m-$BrC_6H_4CH{=}NOC_6H_2$-2,4-$(NO_2)_2$-6-CF_3 (**2d**) 132/8.8/1640. Anal. Calcd for $C_{14}H_7BrF_3N_3O_5$: C, 38.73; H, 1.63; N, 9.68. Found: C, 39.08; H, 1.64; N, 9.76. p-$NO_2C_6H_3CH{=}NOC_6H_2$-2,4-$(NO_2)_2$-6-CF_3 (**2e**) 138-141/9.0/1620. Anal. Calcd for $C_{14}H_7F_3N_4O_7$: C, 42.01; H, 1.76; N, 14.00. Found: C, 41.62; H, 1.58; N, 14.00.

The PhCD=NOAr compounds **1b-3b** were prepared by the reactions of PhCD=NOH with aryl halides. The proton magnetic resonance spectra (acetone-d_6) of PhCD=NOAr were exactly the same as those for PhCH=NOAr (**1a-3a**) except for the complete absence of the benzal C-H singlet of the latter at 8.5-8.8 ppm.

2,4-Dinitroanisole, 2,4-dinitro-6-(trifluoromethyl)anisole, and methyl picrate were prepared by reaction of the appropriate aryl oxide with MeONa-MeOH.

Methanol was purified as described previously. Solutions of MeONa-MeOH were prepared by adding clean pieces of sodium metal to anhydrous MeOH under nitrogen.

X-ray Structure Determination. The X-ray structure determinations of **1a-3a** were performed by Lucky Central Research Institute, Dae Jeon, Korea.

Ultraviolet Spectra of Reaction Products. λ_{max} and molar extinction coefficients of aryl oxides, anisoles, oximes, and Meisenheimer complexes in absolute MeOH were the following: 2,4-dinitrophenoxide, 356 nm (ϵ = 15 400); 2,4-dinitro-6-(trifluoromethyl)phenoxide, 348 nm (ϵ = 16 700); picrate, 354 nm (ϵ = 15 450); 2,4-dinitroanisole, 292 nm (ϵ = 11 200); 2,4-dinitro-6-(trifluoromethyl)anisole, 210 nm (ϵ = 16 400); methyl picrate, 220 nm (ϵ = 17 750); benzaldoxime, 292 nm (ϵ = 13 800); $[(CH_3O)_2C_6H_2$-2,4-$(NO_2)_2$-6-$CF_3]^-$, 472 nm (ϵ = 21 800); $[(CH_3O)_2C_6H_2$-2,4,6-$(NO_2)_3]^-$, 410 nm (ϵ = 24 700); $[(CH_3O)_2C_6H_2$-2,4-$(NO_2)_2$-6-$CF_3]^-$, 472 nm (ϵ = 21 800); $[(CH_3O)_2C_6H_2$-2,4,6-$(NO_2)_3]^-$, 410 nm (ϵ = 24 720).

Kinetic Studies. Reactions of **1-3** with MeONa-MeOH were followed using a Hewlett-Packard 8452 diode array spectrophotometer with thermostated cuvette holders under pseudo-first-order conditions employing at least a 10-fold excess of base. Reactions were initiated by injecting 5-10 μL of an ca. 10^{-2} M solution of substrate in acetonitrile into a cuvette containing 3.0 mL of MeONa-MeOH. Cuvettes were temperature equilibrated for at least 20 min prior to a kinetic run. All reactions were followed to completion. The decreases of the absorptions at 292, 298, and 314 nm for **1**, **2**, and **3**, respectively, with time were monitored. Plots of ln $(A_t - A_\infty)$ against time were linear over at least 2 half-lives or more of the reaction. The slope was the observed rate constant. For reactions of **1** and **2** with MeONa in MeOH, the increase in the absorption at 356 nm was also measured. The rates determined by these two methods were always identical. However, for reactions of **2** at [MeONa] > 0.03 M and of **3** at all base concentrations, the increases in the absorptions of the aryl oxides could not be monitored because the kinetics was complicated by the formation of the Meisenheimer complexes. The observed rate constants were multiplied by the product yields (vide infra) to determine the rate coefficients for the elimination and the S_NAr processes. The k_2^E and k_A values were calculated by dividing the corresponding rate constants by base concentration.

Product Studies. The products of the reactions of **1-3** with MeONa-MeOH were identified as described before.[1,9,12] The yields of the reaction products were determined by comparing the absorbance of the infinity samples from the kinetic reactions with those of authentic samples of the products.

Control Experiments. The stabilities of **1-3** were determined as reported earlier.[1]

Acknowledgment. This research was supported by Non Directed Research Fund, Korea Research Foundation, 1989, KOSEF, and OCRC-KOSEF.

Registry No. 1a, 75735-29-4; **1b**, 139584-37-5; **1c**, 115828-58-5; **1d**, 115828-59-6; **1e**, 75735-26-1; **2a**, 139584-38-6; **2b**, 139584-39-7; **2c**, 139584-40-0; **2d**, 139584-41-1; **2e**, 139584-42-2; **3a**, 115828-60-9; **3b**, 139584-43-3; **3c**, 115828-61-0; **3d**, 115828-62-1; **3e**, 115828-63-2; sodium methoxide, 124-41-4; benzaldehyde oxime, 622-31-1; benzaldehyde-α-d oxime, 14702-03-5; p-methoxybenzaldehyde oxime, 3717-21-3; m-bromobenzaldehyde oxime, 52739-46-5; p-nitrobenzaldehyde oxime, 3717-19-9; 2,4-dinitrophenyl chloride, 97-00-7; 2,4-dinitro-6-(trifluoromethyl)phenyl chloride, 392-95-0; picryl chloride, 88-88-0.

Materials Chemistry of Chiral Macromolecules. 1. Synthesis and Phase Transitions

J. S. Moore and S. I. Stupp*

Contribution from the Department of Materials Science and Engineering and Materials Research Laboratory, University of Illinois at Urbana-Champaign, Urbana, Illinois 61801.
Received November 23, 1990

Abstract: This paper describes work on synthesis of chiral macromolecules as part of a materials chemistry study which seeks to establish links in these systems among molecular structure, three-dimensional molecular organization, and properties. The basic materials chemistry hypothesis driving this work is that chiral forces among stereogenic centers may serve as guiding fields to organize polymers in two or three dimensions. It follows that physical properties could be directly or indirectly controlled by chirality. In order to promote strong forces among chiral centers the chains were designed to have stereogenic carbons substituted by the strongly dipolar cyano group and spaced by 16 atoms along the backbone. The preparative chemistry of chiral macromolecules is challenging given the limited number of polymerization methodologies and the inherent translational periodicity of synthetic polymers. We have synthesized here low symmetry chiral macromolecules in which the only symmetry element retained is polar translation; achiral homologues lacking the nitrile function, the configurationally disordered polymer, and dimeric model compounds were prepared as well. The compounds exhibited crystalline and liquid crystalline phases, and significant differences were observed among homologues through differential scanning calorimetry and optical microscopy. The substitution of nitrile groups every 16 atoms along the polymer backbone, specially with configurational disorder, leads to glassy or less ordered condensed phases. In some polymers when the strongly dipolar stereogenic centers do not have preferred handedness, chains organize into mesophases rather than crystalline structures. This is surprising since the concentration of stereogenic centers is extremely dilute. Using dimeric model compounds, homochiral recognition among stereogenic centers with large dipole moments was identified as an important factor in the assembly of molecules into layered structures. Interestingly, catenation of the dipolar stereogenic centers in polymeric compounds apparently leads to layered structures even when configurational disorder exists along the polymer backbone. This type of structural control could be extremely useful as an approach to tune physical properties of polymeric materials.

Introduction

The combination of chirality and polymeric dimension is ubiquitous in the molecules of nature, yet relatively few synthetic systems have been prepared and studied as three-dimensional molecular assemblies. Such systems have great potential as substrates for the discovery of new phenomena as well as new technically useful solid substances. Because of the many structures that could be achieved through isomeric forms of chiral polymers

0002-7863/92/1514-3429$03.00/0 © 1992 American Chemical Society

in "condensed" states these molecules are excellent for the systematic development of materials chemistry. The basic hypothesis driving our work is that chiral forces among stereogenic centers may not only serve to dictate chain conformation but also serve as guiding fields to organize polymers in two or three dimensions. We therefore infer that chirality in macromolecules could easily couple to other factors and impact on crystallization, phase separation or formation of new phases, vitrification, surface structure, and morphology. It follows that control of physical properties of materials may be directly or indirectly controlled by chirality. Establishing the fundamental links between atomic structure and properties is the common objective of materials science paradigms. This objective has been traditionally pursued in metals and ceramics and to some extent in structurally simple polymers. Given the challenges in preparative chemistry of chiral macromolecules we believe this is one area where chemistry may have great impact in the development of materials science.

Macromolecular chirality has a number of unique features, some related to molar mass and periodicity and others to synthetic methodologies. Defining the existence of chirality in macromolecules it is important to choose a model that ignores chain ends and considers the backbone to be of infinite length. In such a model the existence of chirality is unrelated to molecular size and depends only on the repeat unit structure. The presence of chirality in one-dimensional objects with translational periodicity requires the absence of all symmetry elements of the second kind. Thus, in addition to the absence of improper rotational symmetry which is a sufficient condition for chirality in small molecules, macromolecules also require the elimination of glide-reflection elements. Since periodicity is directly linked to glide-reflection symmetry, it is clear why many stereoregular macromolecules are achiral. For example, the syndiotactic chain contains a glide-reflection axis along the backbone as well as mirror planes perpendicular to the backbone. The classical isotactic chain, on the other hand, illustrates how synthetic methodology limits the construction of chiral polymers. This chain has mirror planes perpendicular to the backbone resulting from periodicity and the common two carbon repeats. Therefore both isotactic and syndiotactic chains contain stereogenic but achirotopic carbons in their backbone. Regiochemical structure, that is the directional relationship among contiguous repeats offers an approach to the construction of chiral chains. The Appendix describes the structure of isoregic, syndioregic, and aregic chains. If one applies the previous symmetry considerations to these structures it is clear that chiral chains can exist in each of the three families. For example, the chiral isoregic structure is the only chiral backbone which possesses a polar translational axis as its only symmetry element. On the other hand, the meso isoregic and meso syndioregic structures are achiral in spite of their complete stereochemical and regiochemical order.

The important and challenging problem which remains largely unexplored in all polymers is an understanding of how chirality can be used to control the three-dimensional organization of macromolecules. Previous work has focused primarily on the conformation of chains in solution[1-4] or the polymerization of conformationally locked chains by chiral initiators.[5,6] One recent study dealt with the synthesis of copolymers in which an asymmetric sequence is assembled by use of a chiral template.[7]

In this work we have designed and constructed a macromolecule which has a chiral isoregic skeleton and probed its structure in the condensed state. Parts of this effort had been described previously in a preliminary paper.[8] The molecule's design included the presence of a chemical function in the stereogenic center with potential to engage in strong intermolecular interactions. The study has also included the synthesis of homologous macromolecules and dimeric model compounds to help us understand the impact of molecular structure in three-dimensional organization of the materials they formed. The repeating units we targeted are shown below, and their selection can be rationalized in the

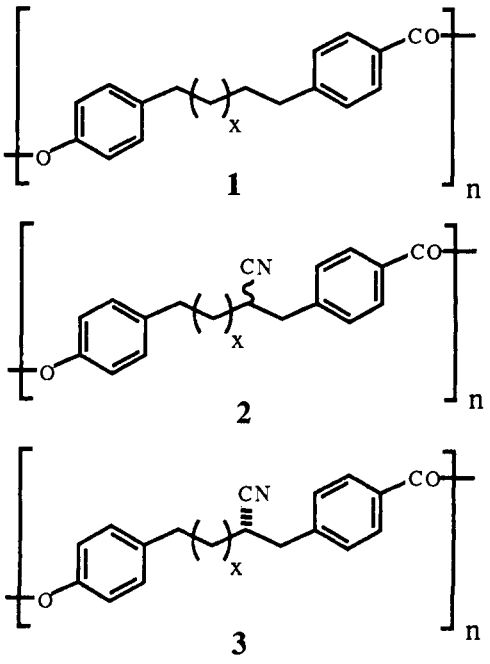

following way. First of all the stereocenter bears the nitrile function, one of the strongest dipoles in organic molecules with a simple structure and well-defined direction. Secondly, because of the para substituted aryl units, parent skeleton **1** has the uniaxal shape characteristic of molecules which form liquid crystalline phases. This was important in our study because we would promote in this way intermediate levels of order between amorphous structures and three-dimensional crystals. Thirdly, this skeleton also possesses polar translational symmetry since it forms by condensation of phenolic and acid functions at opposite ends of its monomeric precursor. The resultant isoregic skeleton removes all reflection elements perpendicular to the main chain axis. Lastly, the purpose of the aliphatic spacer was to obtain soluble and fusible products, two properties which are uncharacteristic of polymers with aromatic backbones. Given the known differences in uniaxial ratio between even- and odd-membered aliphatic sequences we chose to include in our study both a hexyl and a heptyl spacer group. Polymer **2** represents the product from polymerization of the racemic monomer, and it is therefore an aperiodic chain with respect to configuration at the stereocenter. This system is best described as a set of diastereomeric chains and not as a true racemate since a complete set of stereoisomers in Bernoullian polymers of finite length cannot be generated.[9] The system associated with structure **3** represents a pure enantiomer.

Results and Discussion

Synthesis of Polymeric Compounds. Polyesters **1–3** were derived from self-condensation of their corresponding hydroxyacid monomers. Prior to our work few methods were known to yield high molar mass polymers directly from hydroxyacid monomers or their derivatives.[10] Moreover, the anticipated sensitivity of the nitrile

(1) Pino, P. *Adv. Polym. Sci.* **1965**, *4*, 236.
(2) Goodman, M.; Abe, A.; Fan, Y. L. *Makromol. Rev.* **1966**, *1*, 1.
(3) Ciardelli, F.; Chiellini, E.; Carlini, C. In *Optically Active Polymers*; Selegny E., Ed.; Reidel: Dordrecht, 1979; p 83.
(4) Green, M. M.; Andreola, C.; Munoz, B.; Reidy, M. *J. Am. Chem. Soc.* **1988**, *110*, 4063.
(5) Okamoto, Y.; Suzuki, K.; Ohta, K.; Hatada, K.; Yuki, H. *J. Am. Chem. Soc.* **1979**, *101*, 4763.
(6) Vogl, O.; Jaycox, G. D.; Xi, F.; Hatada, K. *Polym. Prepr. Am. Chem. Soc. Div. Polym. Chem.* **1989**, *30*, 435 and references therein.
(7) Wulff, G.; Kemmerer, R.; Vogt, B. *J. Am. Chem. Soc.* **1987**, *109*, 7449.
(8) Stupp, S. I.; Moore, J. S.; Li, L. S. *Polymer Preprints* **1989**, *30(2)*, 396.
(9) Green, M. M.; Garetz, B. A. *Tetrahedron Lett.* **1984**, *25*, 2831.
(10) (a) Higashi, F.; Yamada, Y.; Hoshio, A. *J. Polym. Sci., Polym. Chem. Ed.* **1984**, *22*, 2181. (b) Higashi, F.; Akiyama, N.; Takahashi, I. *J. Polym. Sci., Polym. Chem. Ed.* **1984**, *22*, 1653. (c) Higashi, F.; Takahashi, I.; Akiyama, N. *J. Polym. Sci., Polym. Chem. Ed.* **1984**, *22*, 3607. (d) Higashi, F.; Mashimo, T.; Takahashi, I.; Akiyama, N. *J. Polym. Sci., Polym. Chem. Ed.* **1985**, *23*, 3095. (e) Kricheldorf, H. R.; Zang, Q.-Z.; Schwarz, G. *Polymer* **1982**, *23*, 1821.

stereocenter toward racemization required mild polymerization conditions. These difficulties were overcome in our recently developed polymerization methodology for direct condensation of phenolic acids at room temperature and neutral pH.[11] Most importantly we showed that under these conditions racemization at the nitrile stereocenter did not occur. The control of absolute stereochemistry at the nitrile α-carbon was accomplished through Ender's asymmetric alkylation chemistry[12] followed by our own methodology for hydrazone to nitrile functional group conversion which conserves stereochemical purity.[13] The homologues lacking the strong dipole required eight steps and were obtained in overall yields ranging from 8.5 to 15.8%. Macromolecules containing the chiral nitriles required 14 steps and were obtained in 4.1–8.2% yields. Materials containing enantiomerically enriched chains were prepared in scales of several hundred milligrams, and all other products were prepared in gram quantities. The highest ee values obtained in the enantiomerically enriched materials was in the order of 0.87. These values were measured through isotope labeling experiments which are briefly discussed below.

The weak acidity of the nitrile α-proton made it essential to determine the extent of racemization during deprotection of nitriles **4** and during the subsequent polymerization. Since the specific rotations of these compounds are not known, an absolute method for determination of the ee was necessary. The enantiomeric purity of **4** was already known, and it was possible to monitor changes in stereochemistry which resulted from the transformation of **4** to **3**. Assuming that racemization during deprotection and polymerization would involve proton exchange at the nitrile α-carbon, isotope labeling was judged to be the most effective way to monitor changes in enantiomeric purity. This assumption is reasonable since all reactions from **4** to the final target polymers require mildly acidic or basic reagents and proton sources for exchange are potentially available. Compounds **4** as well as monomers **5** are ideally suited for the labeling experiments since deuterium introduction at the α-carbon can be easily accomplished by proton-deuterium exchange. Our idea was to track the isotope abundance at the α-carbon for **4** after the various chemical transformations in order to quantify enantiomeric excess. Following chromatographic purification the isotope abundance of the labeled compound was measured by mass spectrometry and the site of label incorporation was determined by ^{1}H NMR. The main isotopic species, present at a level of 93%, was found to contain three deuterium atoms per molecule. Because only a weak molecular ion peak could be observed for this compound the error in this value is estimated to be ±3–5%. ^{1}H NMR showed that incorporation of the label occurred exclusively at the nitrile α-carbon and also at the benzylic position para to the *tert*-butyl ester (no exchange was observed at the benzylic position para to the silyl ether). This selectivity must arise from electronic differences in the two aryl units.

Under the conditions used silyl ether cleavage occurred rapidly (30 min) and in good yield. When (±)-**4a**-d_3 was subjected to these conditions, the resulting phenol was found to be trideuterated to a level of 88% by mass spectrometry. This value falls nearly within the error limits of the percent measured for (±)-**4a**-d_3. Thus it is difficult to determine precisely the extent, if any, of racemization, but clearly it is no more than 5% for the desilylation step. The conditions used to remove the *tert*-butyl group could promote racemization at the nitrile α-carbon. Clearly if this were to occur deuterium-proton exchange in (±)-**4a**-d_3 would be observed. As seen in Scheme III, however, this was found not to be the case. In fact, the percent of trideuterated species in the resulting (±)-**5a** was found to be slightly greater than that measured for (±)-**6a**-d_3 but still within the limits of experimental error. Again, little or no racemization was believed to occur during the cleavage of the *tert*-butyl ester with TFA. Overall, it was concluded that less than 5% racemization took place during the two-step deprotection sequence. Finally, we had previously shown with similar labeling experiments that no racemization occurs during the carbodiimide polymerization used to construct the target polymers.

Phase Transitions of Polymeric Compounds. Figure 1 shows DSC traces of the six polymers synthesized, and Table I lists all the temperatures, enthalpies, and entropies associated with the phase transitions observed. When nitrile groups substitute the chains either with or without configurational bias, the DSC indicates a decrease of molecular order in the condensed phases of these polymers. This is reflected in different ways depending on the structure of repeating units. In the case of odd polymers **2b** and (*S*)-**3b** ($x = 4$) the DSC trace shows a remarkable decrease of order, revealing only a glass transition temperature near 80 °C which is not sensitive to configuration. In great contrast the corresponding parent polymer lacking dipolar substitution yields a crystalline polymer as indicated by the well defined DSC endotherm at the melting point. Frustration of three-dimensional order is clearly brought about by the strong dipolar forces among chains. It is very surprising to observe this frustration of three-dimensional order given that stereogenic centers containing the strong dipole are spaced by 16 atoms along the molecular backbone. The great resistance to ordering in the configurationally disordered polymer **2b** is also revealed by observations reported in Table II. Melts of this polymer do not reveal any significant shear-induced long range molecular orientation commonly observed in polymers as optically visible birefringence. In contrast the enantiomerically enriched macromolecules with odd spacer do order upon shearing, forming a strongly birefringent medium. This birefringence is lost irreversibly upon further heating of samples into the range 160–190 °C. The observations represent an additional indication that in the odd-spacer polymers ordering is frustrated by the stereochemical disorder of dipoles.

In even-spacer polymers **1a**, **2a**, and (*S*)-**3a** ($x = 3$) the decrease in order with dipolar substitution is revealed by their relative isotropization temperatures. In the parent polymer lacking the dipolar stereogenic centers isotropization occurs at the highest temperature among the three polymers. The enthalpy and entropy associated with the isotropization transition are also highest in the parent polymer. On the basis of the information summarized in Table II the first phase transition of the parent polymer with the even spacer corresponds clearly to a crystal to liquid crystal transition. In fact the texture observed above melting is characteristic of a smectic phase.

Both the configurationally enriched and the configurationally disordered polymers **2a** and (*S*)-**3a** having even spacers did organize into ordered structures as revealed by well defined DSC endotherms. However, the enantiomerically enriched polymer always revealed two endotherms, and only a single one was observed in the racemate. The evolution of the DSC trace from a single to a double endotherm as stereochemical order increases is clearly revealed by the curves of Figure 2. The temperatures associated with both melting peaks are plotted in Figure 3 as a function of ee value in the system and Figure 4 shows the total values of ΔH and ΔS for the high temperature transitions. It is interesting to observe that the racemate's single endotherm occurs at a temperature which is higher than that of both endotherms in the system with an ee value of 49%.

The room temperature micrographs of **2a** and (*S*)-**3a** shown in Figure 5 reveal the grainy texture characteristic of crystalline materials in the enantiomerically enriched polymer and for the racemate the smoother but strongly birefringent texture one would expect from a vitrified liquid crystalline phase. One may therefore assume that in materials with enantiomeric bias the low temperature peak represents the melting of three-dimensional order into a mesophase. In this context the decreasing temperature of the crystal to mesophase transition as ee values get lower is expected since crystals must accommodate more configurational disorder. Similarly the isotropization temperatures are expected to decrease if order in the mesophase correlates with order in the

(11) Moore, J. S.; Stupp, S. I. *Macromolecules* **1990**, *23*, 65.
(12) (a) Enders, D. In *Asymmetric Synthesis*; Morrison, J. D., Ed.; Academic Press: New York, 1984; Vol. 3, Chapter 4. (b) Enders, D. *Nach. Chem. Tech. Labor.* **1984**, *33*, 882. (c) Enders, D. In *Selectivity—A Goal for Synthetic Efficiency*; Trost, B. M., Bartmann, W., Eds.; Verlag Chemie: Weinheim, 1984; p 65.
(13) Moore, J. S.; Stupp, S. I. *J. Org. Chem.* **1990**, *55*, 3374.

Scheme I

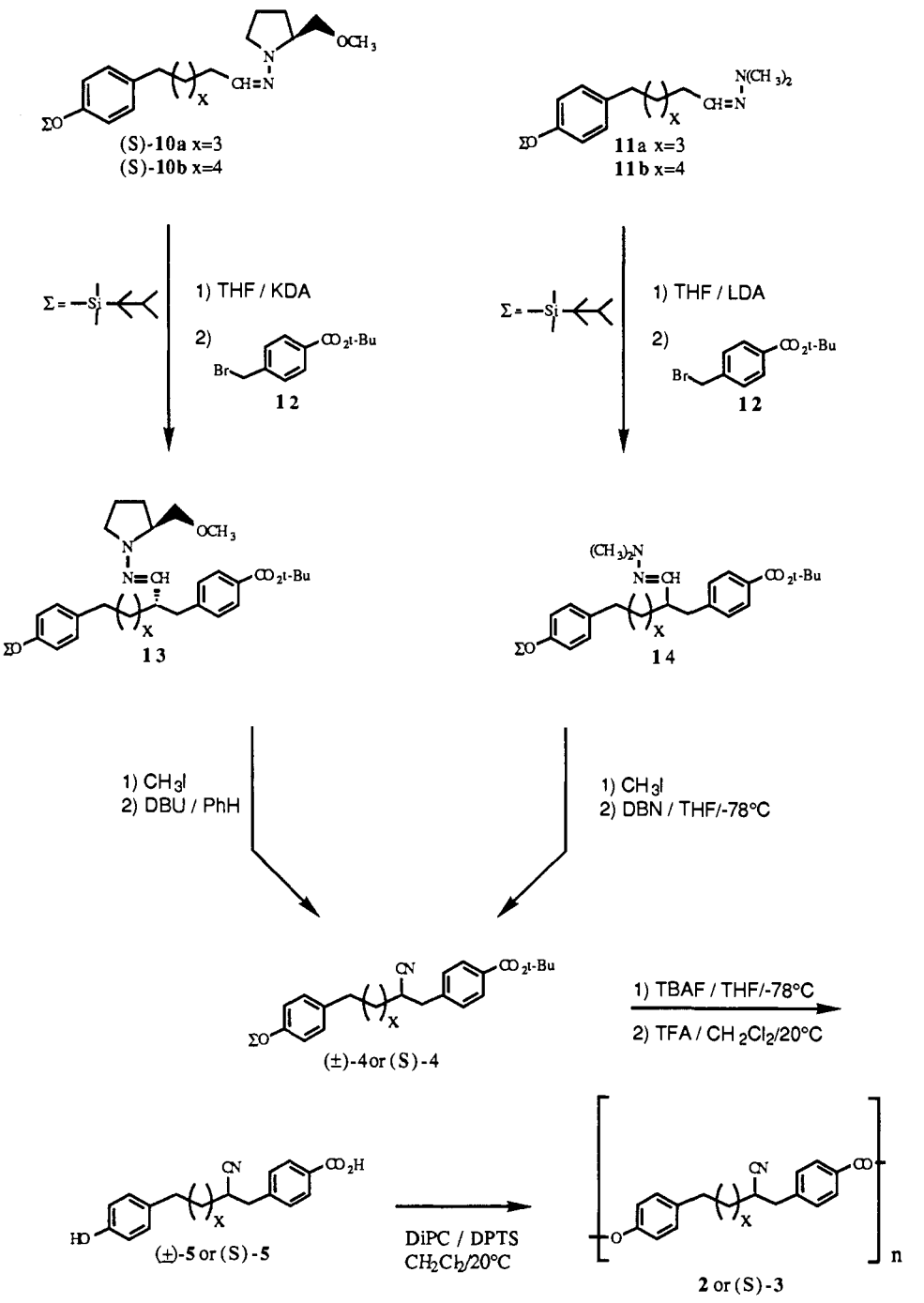

Scheme II

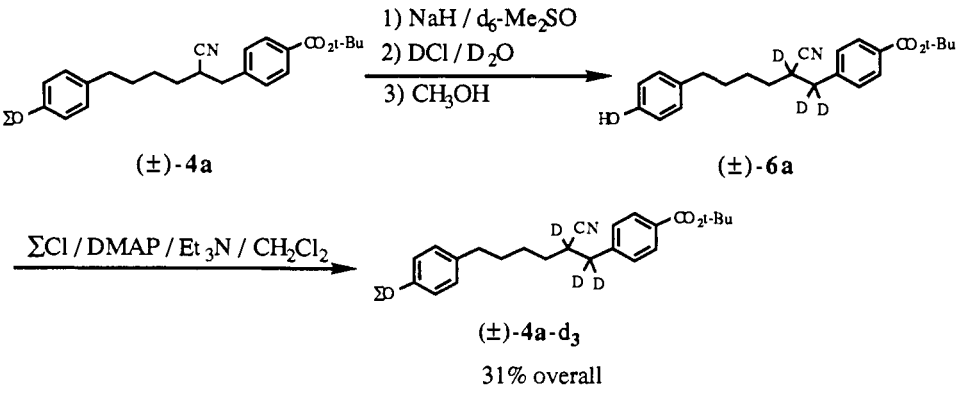

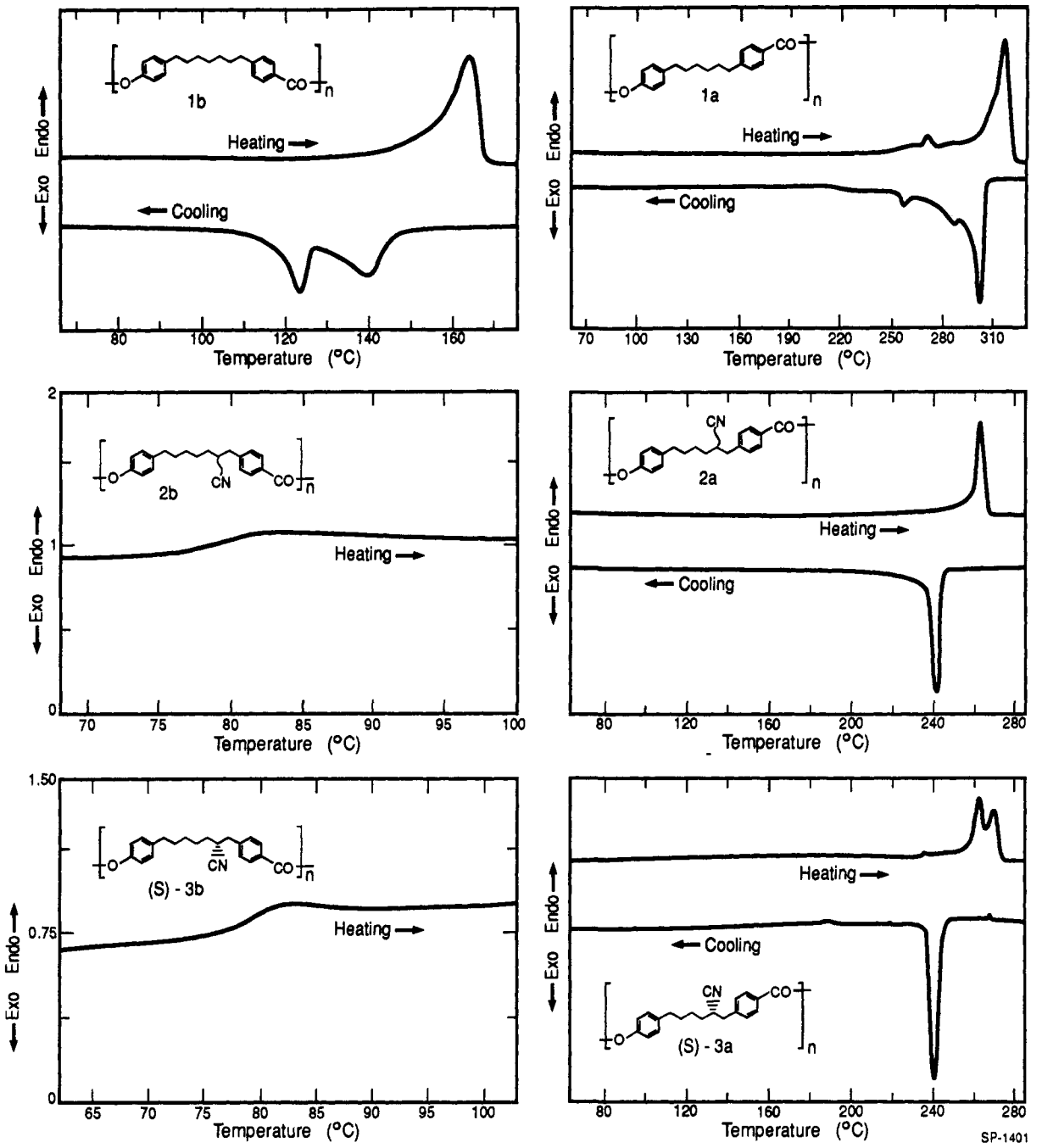

Figure 1. Differential scanning calorimetry scans of homologous polymers.

Scheme III

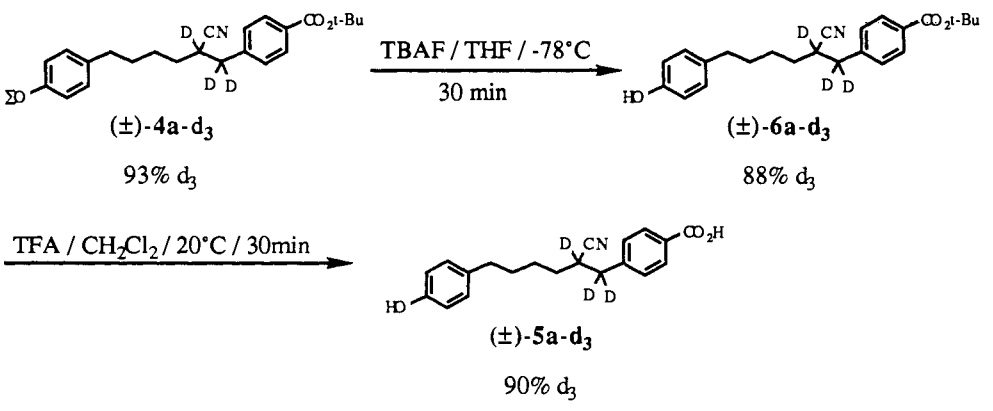

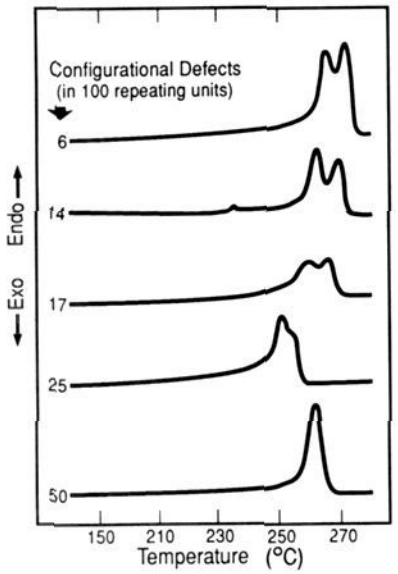

Figure 2. Differential scanning calorimetry scans of polymers with increasing degrees of enantiomeric enrichment.

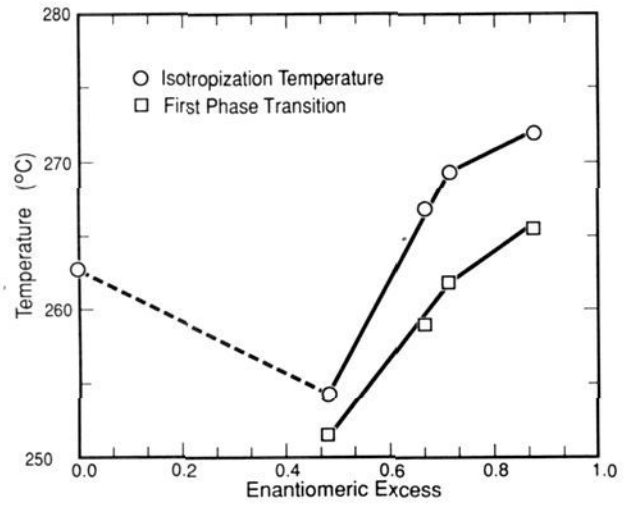

Figure 3. Transition temperatures of polymers varying in values of enantiomeric excess.

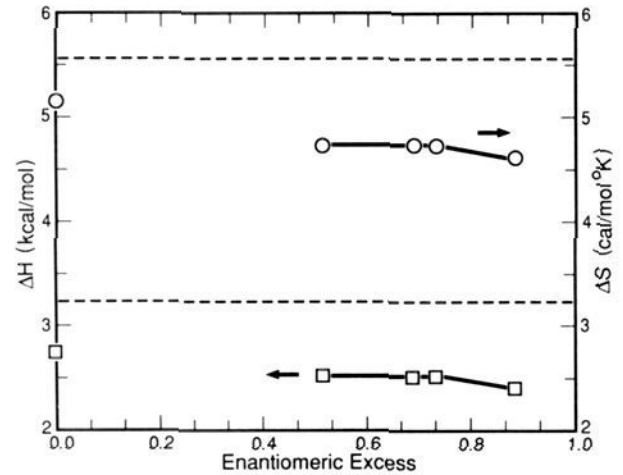

Figure 4. Total enthalpies and entropies of transition in polymers with even spacer having different values of enantiomeric excess.

crystalline state. However it is not clear why configurationally disordered diastereomeric chains have a higher isotropization temperature than some systems with enantiomerically enriched chains. Generally speaking it is interesting that in the absence

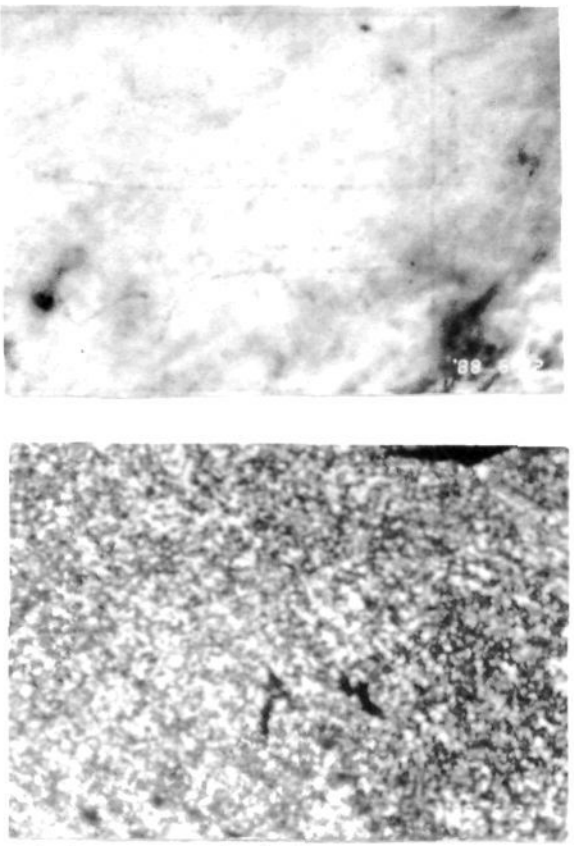

Figure 5. Optical micrographs of solid materials at room temperature using a magnification of 320×. The top micrograph corresponds to the polymeric racemate **2a** and the bottom one to the enantiomerically enriched analogue (*S*)-**3a**.

of preferred handedness a dilute concentration of dipolar stereogenic centers along the backbone keeps the system organized as a mesophase and not as a crystalline phase. This is interesting in the context that nonstereoregular polymers are known which form "crystalline" phases, and yet every other carbon in their backbone is stereogenic (e.g., poly(vinyl alcohol) and poly(vinyl fluoride).[14] The great sensitivity of the structure to stereochemical disorder found here must be linked to the strong dipole moment associated with the stereogenic center.

Phase Transitions of Dimeric Model Compounds. In order to gain further understanding of the polymeric materials studied here we synthesized and analyzed the phase transitions of compounds containing a single stereogenic center, one racemic and the other enantiomerically enriched. Racemic compound (±)-**7** and enantiomerically enriched compound (*S*)-**7** were chosen as small molecule models for polymers **2a** and (*S*)-**3a**, respectively. These structures closely resemble the dimeric repeat unit of their corresponding polymers except that only a single nitrile group is present in the model compounds.

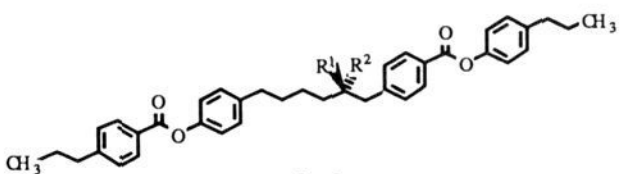

(±)-**7** $R^1, R^2 = -CN \Leftrightarrow -H$

(S)-**7** $R^1 = -H$, $R^2 = -CN$

Figure 6a shows the DSC scan of solution grown crystals from the racemic compound (±)-**7** revealing two main phase transitions

(14) Wunderlich, B. *Macromolecular Physics*; Academic Press: New York, 1973; Vol. 1, p 151.

Table I. Temperatures, Enthalpies, and Entropies of Transition for the Homologous Series of Polymers

polymer	temp[a] (°C)	ΔH (kcal mol^{-1})	ΔS (cal mol^{-1} K^{-1})
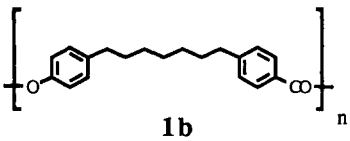 **1b**	155	1.6	3.6
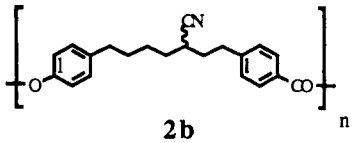 **2b**	80[b]		
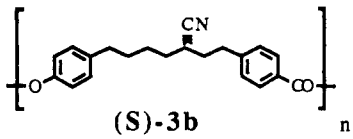 **(S)-3b**	80[b]		
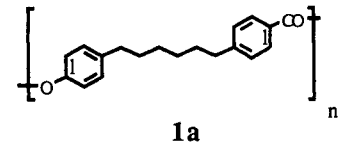 **1a**	268	0.1	0.1
	308	3.2	5.5
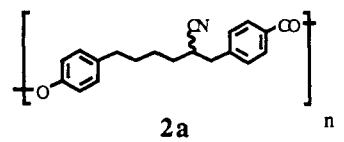 **2a**	263	2.8	5.1
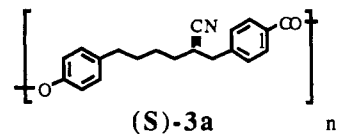 **(S)-3a**	266	2.4[d]	4.6[d]
	272		

[a] Onset temperatures. [b] Glass transition temperature. [c] ee = 0.88. [d] Total value for both phase transitions.

at 107 and 126 °C. On the basis of observations by optical microscopy the first of these two transitions is a crystal-to-liquid crystal transition and the second is an isotropization transition. A DSC scan of the enantiomerically enriched compound (*S*)-**7** is shown in Figure 6b and reveals different behavior. In this case there is effectively one phase transition observed on heating at 116 °C (the very small endotherm at 98 °C is possibly a solid–solid transition). One possible reason for the broadness of the phase transition is the limited optical purity of this compound (0.7–0.85 ee). However upon cooling both the racemic and enantiomerically enriched compounds reveal two phase transitions. This implies that the enantiomer is monotropic (liquid crystallinity is only observed on cooling) and that its crystals have greater thermal stability relative to those formed from the racemate. It is fascinating that a striking difference exists between the liquid crystalline textures of the two model compounds. On the basis of the textures observed by optical microscopy a possible interpretation is that molecules in the enantiomerically enriched compound organize into layers given the easily recognized smectic texture in Figure 7a. The observed phase may also be cholesteric since the textures of some cholesteric phases can be similar to those of smectics. However, in these cases the cholesteric may be strongly twisted, and the phase can be considered to have a quasi-layered structure.[15] *When the only stereogenic center in the rather large dimeric molecule no longer has a dipole moment with "preferred handedness" the layered organization seems to be lost. Instead simple nematic order occurs implying that homochiral recognition among the strong dipoles plays a critical role in assembling molecules into layers.* Another perspective would be to state that if molecules of this specific racemate were to organize into a smectic phase strong electrostatic repulsions among heterochiral centers would destabilize the molecular layers. Given the extended shape of the molecule the alternative organization is nematic order in which molecules are simply orientationally ordered. The nematic order in the racemate is inferred from the nature of the texture (see Figure 5b) and the low enthalpy of the isotropization transition, within the 0.02–2.1 kcal/mol range observed for low molar mass nematogens.[16] A very interesting observation is the fact that upon heating the ensemble of enantiomerically enriched dimers melts into an isotropic liquid at a temperature where the racemate remains organized as a nematic liquid crystal. One may speculate that the tendency of molecules to form layered structures through homochiral recognition demands a high entropy cost and the ensemble thereby favors isotropization. In contrast the higher entropy of the nematic phase stabilizes orientational order in the racemic ensemble.

An additional difference between the model compounds is the greater tendency of the enantiomer to crystallize compared to the racemic mixture. This is obvious from the greater supercooling observed by DSC in the racemate (41 °C) relative to the enantiomerically enriched compound (27 °C) (Figure 6a,b). Also, incomplete crystallization in the racemate is suggested by the inequality between heat acquired and heat released during heating and cooling cycles. Finally the photographs in Figure 8 show the contrast between the two compounds at various temperatures. The enantiomerically enriched one crystallizes into well developed spherulites within the range 96–75 °C, while the racemate still retains a liquid crystalline texture.

Polymeric vs Dimeric Compounds. The higher phase transitions observed in polymeric as opposed to dimeric compounds were assumed to result directly from higher molar mass. This was confirmed by the synthesis of three different racemic compounds

(15) Demus, D.; Richter, L. *Textures of Liquid Crystals*; Verlag Chemie: Weinheim, New York, 1978; p 49.

(16) Beguin, A.; Dubois, J. C.; Le Barny, P.; Billard, J.; Bonamy, F.; Buisine, J. M.; Cuvelier, P. *Mol. Cryst. Liq. Cryst.* **1984**, *1*, 115.

Table II. Summary of Observations by Optical Microscopy

polymer	T_1[a] (°C)	T_2[b] (°C)
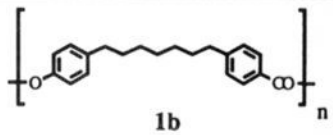 **1b**	*c*	178
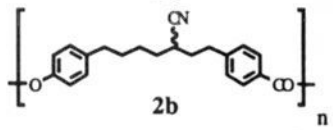 **2b**	*d*	*d*
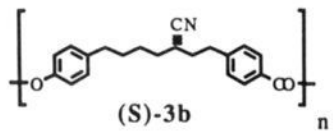 **(S)-3b**	*c*	160–190[e]
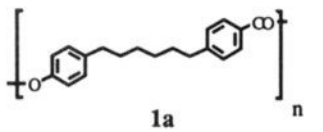 **1a**	280	333
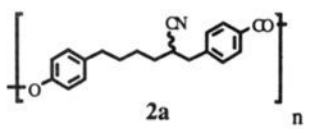 **2a**	*c*	277
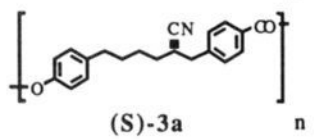 **(S)-3a**	*c*	284

[a] Temperature at which the solid becomes a deformable birefringent medium. [b] Temperature at which birefringence disappears. [c] Not observable. [d] Absence of birefringence at any temperature. [e] Birefringence observed after shearing disappears in this temperature range (little birefringence is observed in **2b**).

with gradually increasing molecular weight. These compounds of intermediate molar mass are described in Table III and were prepared with varying quantities of the monofunctional reagent 4-propylphenol. In the limit of complete conversion their respective degrees of polymerization $\bar{X}_n$ should have values given by

$$\bar{X}_n = l + r$$

where r is the molar ratio of bifunctional to monofunctional monomer. Following polymerization the terminal phenolic groups were capped with 4-propylbenzoic acid in order to stabilize the chains against transesterification reactions.[17] Table III also shows the values of $\bar{X}_n$ calculated from the end group analysis by ^{1}H NMR and they are in satisfactory agreement with those calculated by the expression above. All the compounds of intermediate molar mass formed liquid crystalline fluids of high viscosity, and it is therefore very likely that they form smectic phases. Their transition temperatures are given in Table III and confirm that the higher phase transition temperatures in polymeric compounds are the result of larger molar mass.

The observation of birefringent fluids in low molecular weight racemic polymers confirms the earlier suggestion that liquid crystallinity occurs in the high molar mass compound. Furthermore the high viscosity in low molecular weight polymers indicates that a smectic rather than nematic assembly of molecules probably occurs in the racemic polymer. Given that the racemic model compound melts into a nematic assembly the implication is that catenation of 5–50 or more stereogenic centers into diastereomeric chains once more promotes a layered organization of molecules. This issue is explored further in the next paper of the series dealing specifically with three-dimensional organization

(17) Wu, J.; Stupp, S. I. *Disordering of a Chemically Periodic Chain: Transesterification of a Nematogen*; submitted for publication.

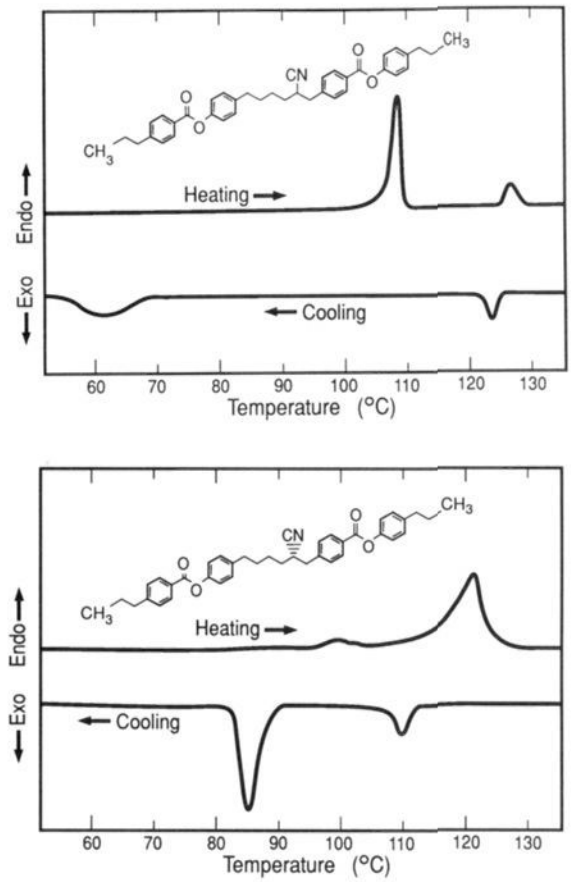

Figure 6. Differential scanning calorimetry of (a) the racemic model compound (solution crystallized) and of the melt crystallized enantiomeric model compound (b).

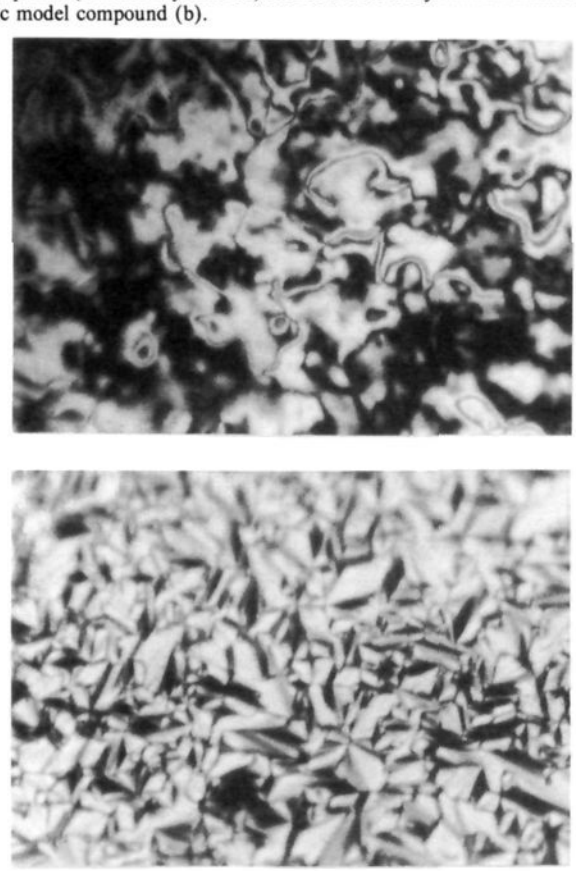

Figure 7. Optical microscopic texture of the racemic model compound (top) and the enantiomeric model compound (bottom) (320× magnification).

Scheme IV

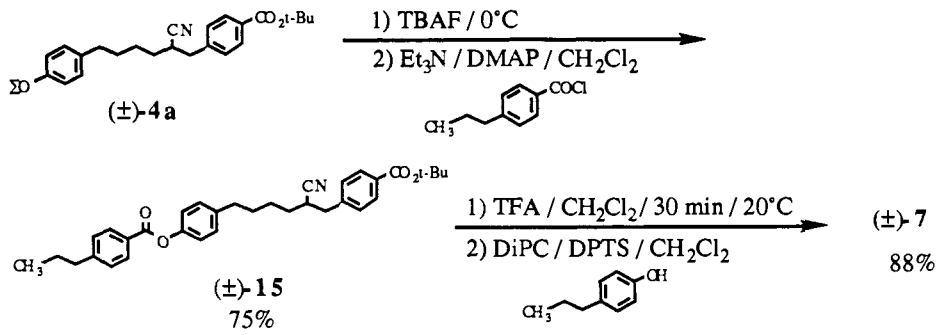

Table III. Compounds of Intermediate Molar Mass

r^a	$\bar{X}_n$(calcd)	$\bar{X}_n$(obsd)[b]	transition[c] temp (°C)	ΔH^d (kcal mol^{-1})	T_1^e (°C) (see text)	T_2^f (°C) (see text)
4.0	5.0	5.1	204	−1.2	170	230
9.0	10.0	9.1	222	−2.0	205–210	249
19.0	20.0	15.5	233	−2.2	195–205	254

[a] Molar ratio of bifunctional to monofunctional monomer. [b] ^{1}H NMR analysis of end groups. [c] Onset of main exotherm upon cooling. [d] Enthalpy measured upon cooling. [e] See *a* in Table II. [f] See *b* in Table II.

Table IV. Monomers Containing CN Dipoles in a Stereogenic Center

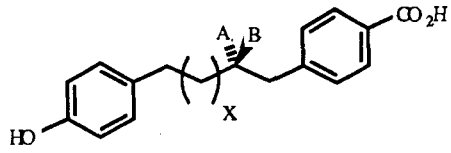

monomer	−A	−B	x
(*S*)-**5a**	−H	−CN	3
(*R*)-**5a**	−CN	−H	3
(±)-**5a**	−H, −CN	−CN, −H	3
(*S*)-**5b**	−H	−CN	4
(*R*)-**5b**	−CN	−H	4
(±)-**5b**	−H, −CN	−CN, −H	4

of the molecules. Finally it is interesting that in great contrast to the behavior of the dimers, the polymeric compound with highest ee value undergoes isotropization at a temperature which is significantly higher than that of the racemate. The opposite behavior observed in the dimer, namely, lower isotropization temperature in the enantiomeric compound, could be based on the high entropy cost involved in keeping the dimeric system organized as a layered mesophase. In this context the entropy change in the polymeric compound between the layered mesophase and the isotropic state would not be as great as it is in the dimer. Using a similar argument one could understand why transition temperatures pass through a minimum as enantiomeric enrichment is increased. The stability of the ordered structure in the polymeric racemate relative to the system with slight enantiomeric enrichment could be explained by additional conformational entropy linked to stereochemical disorder. This additional entropy would disappear gradually with enantiomeric enrichment of the molecular backbone thus destabilizing the ordered mesophase.

Conclusions

We have synthesized low symmetry chiral macromolecules in which the only symmetry element retained is polar translation. A special feature of these chains is the presence of the strongly dipolar cyano group in stereogenic centers spaced by 16 atoms along the backbone. We also synthesized achiral homologues lacking the nitrile function and the configurationally disordered racemic system. The substitution of the large dipoles every 16 atoms along the polymer backbone, specially with configurational disorder, leads to glassy solids or less ordered condensed phases. In some polymers when the strongly dipolar stereogenic centers do not have preferred handedness, chains organize into mesophases rather than crystalline structures. This is surprising since the concentration of stereogenic centers is extremely dilute. Using dimeric model compounds, homochiral recognition among stereogenic centers with large dipole moments was identified as an important factor in the assembly of molecules into layered structures. Interestingly, catenation of the dipolar stereogenic centers in polymeric compounds apparently leads to the layered structures even when configurational disorder exists along the polymer backbone. Our observations demonstrate that the stereochemistry of strongly dipolar chiral centers is very effective in controlling intermediate levels of order in polymeric materials. This type of structural control could be extremely useful as an approach to tune their physical properties.

Experimental Section

Synthesis of Polymeric Compounds. Synthesis of parent monomers **8** required large quantities of substituted acids **9a** and **9b**. Synthesis of

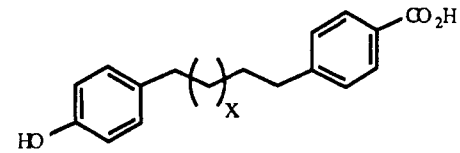

8a x=3
8b x=4

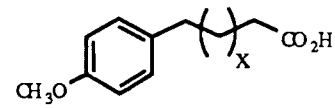

9a x=2
9b x=3
9c x=4

aryl pentanoic acid **9a** began by addition of the Grignard reagent prepared from *p*-bromoanisol to cyclopentanone. Following spontaneous dehydration, oxidative cleavage of the cyclopentene using RuO_4,[18] gave the ketoacid in 35% yield for the two steps. The ketoacid used as the precursor of **8b** was prepared by 5-carbon atom homologation of *p*-anisic acid. Thus, the acylation product prepared by reacting *p*-anisoyl chloride and 1-morpholino-1-cyclopentene was subjected to forcing acidic hydrolysis to give directly the ketoacid in 30.5% overall yield. These reactions could conveniently be conducted on a half-mole scale, so that 50-g quantities of the ketoacid could be routinely obtained. Wolff–Kishner reduction of ketoacids under standard Huang-Minlon conditions gave crystalline acids **9a** and **9b** in 89% and 72% yields, respectively.[19]

(18) Carlsen, H. J.; Tsutomu, K.; Martin, V. S.; Sharpless, K. B. *J. Org. Chem.* **1981**, *19*, 3936.
(19) Huang-Minlon *J. Am. Chem. Soc.* **1946**, *68*, 2487.

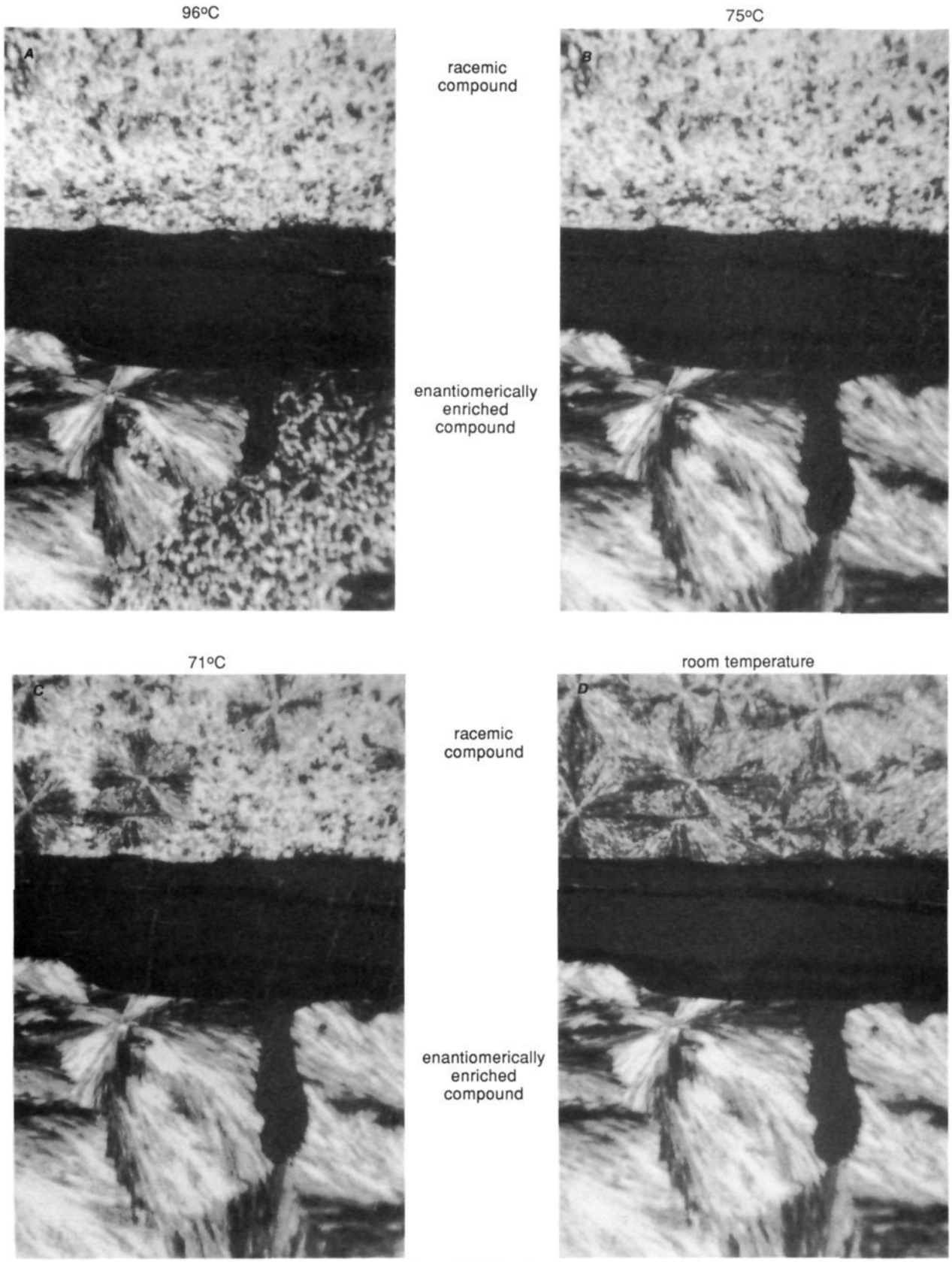

Figure 8. Optical micrographs obtained at 96 °C (A), 75 °C (B), 71 °C (C), and room temperature (D) during the crystallization of the racemic (top) and enantiomeric (bottom) model compounds (200× magnification).

Acids **9a** and **9b** were reduced directly to their alcohols with lithium aluminum hydride ($LiAlH_4$) in 89–91% yield. Without further purification, the alcohols were converted to bromides using triphenylphosphine/carbon tetrabromide reagent.[20] The bromides were isolated as colorless liquids in 83–91% yield by fractional distillation. Alkylation of the dianion of *p*-toluic acid[21] with the bromides gave methoxyether derivatives in 62–66% yield. Demethylation with HBr proceeded without difficulty to give parent monomers **8** as crystalline solids. Finally, car-

(20) For a review, see: Appel, R. *Angew. Chem., Int. Ed. Eng.* **1975**, 801.

(21) Creger, P. L. *J. Am. Chem. Soc.* **1970**, *92*, 1396.

Scheme V

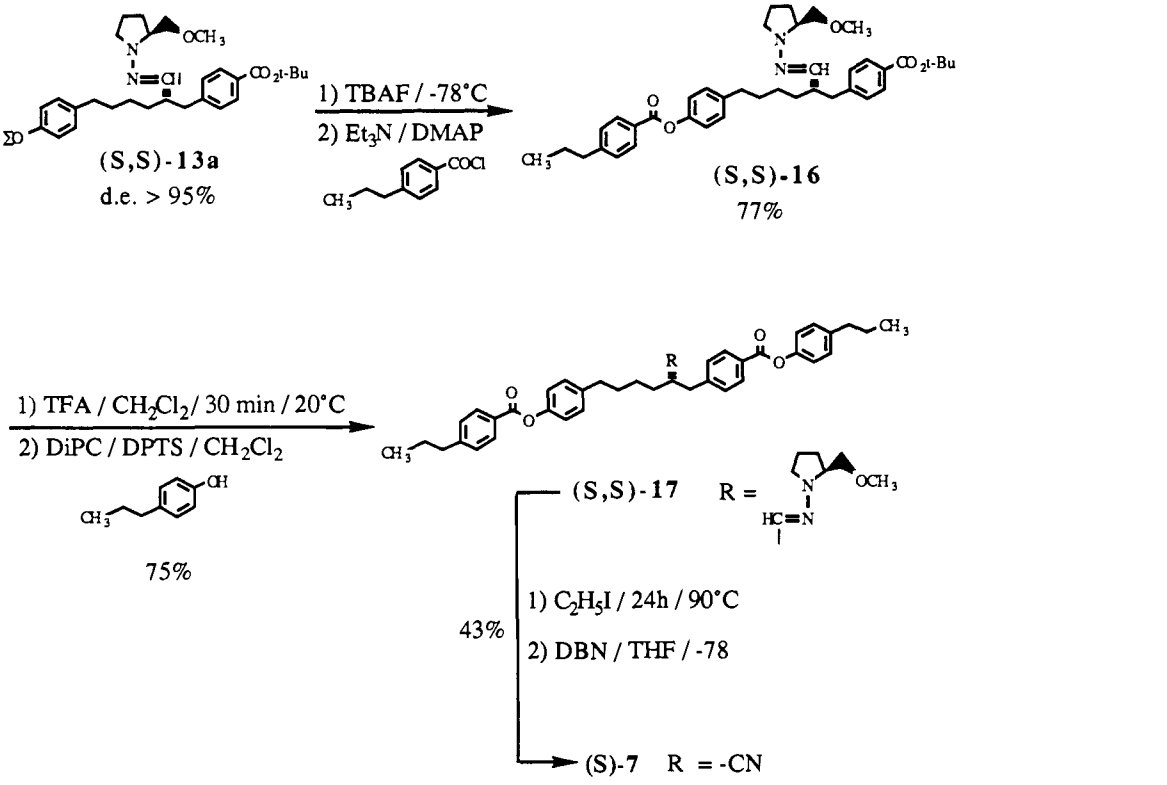

bodiimide-based polyesterification of monomers **8** using our room temperature conditions gave parent polymers **1** in high yield with degree of polymerization greater than 50.

The synthesis of monomers **5** described in Table IV started with demethylation of **9** with hydrobromic acid in refluxing acetic acid to give the phenol as a crystalline solid in 89–92% yield. Next, the carboxylic acid group was temporarily protected as its ethyl ester and without further purification the phenolic group was protected as its thexyldimethylsilyl ether. The protected compound was prepared in 84–93% yield by reaction of thexyldimethylsilyl chloride in methylene chloride using triethylamine and catalytic quantities of DMAP.[22] The analytically pure product was recovered as a colorless oil after purification by either fractional distillation or silica gel chromatography. At this point, the oxidation level at the carbonyl carbon was adjusted by a reduction–oxidation sequence. Lithium aluminum hydride reduction gave the corresponding alcohol as a colorless oil in 91–98% yield. Without further purification, the crude alcohol was oxidized to the aldehyde using pyridinium chlorochromate[23] (PCC) in methylene chloride. A 74–77% yield of analytically pure aldehyde was achieved from the ester following purification by silica gel chromatography.

At this point, the aldehyde was reacted with different amines depending on the configuration desired at the nitrile α-carbon. Thus, monomer (*R*)-**5** was derived from RAMP hydrazone (*R*)-**10**, monomer (*S*)-**5** from SAMP hydrazone (*S*)-**10**, and racemic monomer (±)-**5** from *N*,*N*-dimethylhydrazone (DMH), **11**. These hydrazones were prepared from aldehydes by standard methods.[12] Chromatographic purification left analytically pure hydrazones **10** and **11** as colorless oils in 88–97% yield.

Alkylation of hydrazones **10** and **11** with *tert*-butyl 4-α-bromotoluate **12** gave hydrazones **13** and **14** as shown in Scheme I. This useful alkylating agent could be prepared in multigram quantities by benzylic bromination of the known *tert*-butyl-*p*-toluate.[24] DMHs anion generation was best accomplished with KDA. On the other hand, metalation of SAMP and RAMP hydrazones was successfully performed with a 0.3 M solution of LDA in THF (1.0 equiv). Alkylation of these species with **12** gave reasonably high yields of **13** and **14**. Moreover for **13** only a single diastereomer was observed. Diastereomeric excess of **13** was conveniently measured by ^{1}H NMR spectroscopy. For this purpose, the 1:1 diastereomeric mixture of (*S*,*S*)-**13** and (*S*,*R*)-**13** was prepared from the racemic DMH **14**. Thus, hydrolysis of the methiodide derivatives of (±)-**14** gave the corresponding racemic aldehydes in 31–67%. A 1:1 diastereomeric mixture of SAMP hydrazones was then obtained in 65–77% by reaction of these aldehydes with SAMP hydrazine. The ^{1}H NMR spectrum of this mixture showed a pair of well resolved singlets corresponding to the diastereomeric methoxy groups. It was not possible to measure de accurately using these resonances due to the presence of several less intense multiplets in this region of the spectrum (a reliable baseline could not be established). Instead it was found that homonuclear decoupling of the methine resonance collapsed the formyl proton triplet

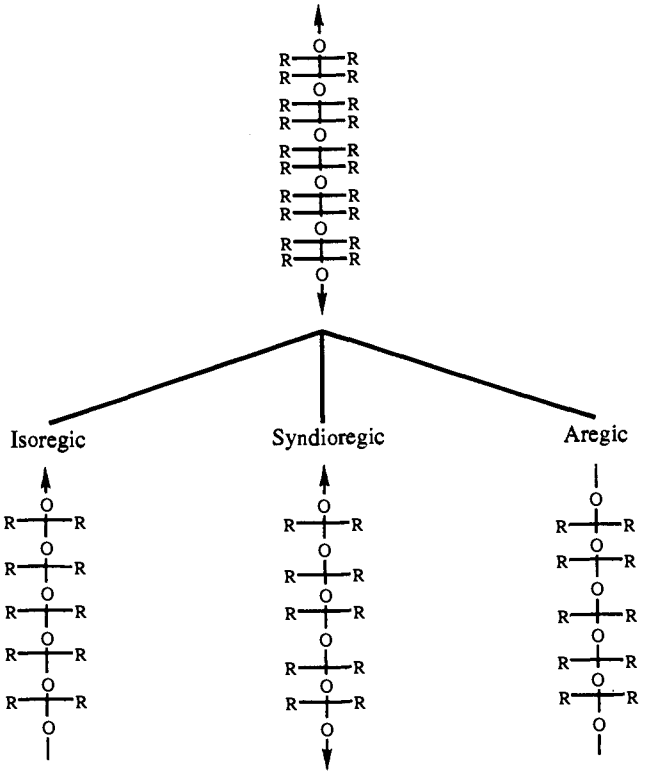

Figure 9. Structural forms of condensation macromolecules at the level of regiochemical order.

(22) Wetter, H.; Oertle, K. *Tetrahedron Lett.* **1985**, *26*, 5515.
(23) Corey, E. J.; Suggs, J. W. *Tetrahedron Lett.* **1975**, 2647.
(24) Hunig, S.; Lucke, E.; Brenninger, W. In *Organic Syntheses*; Wiley: New York 1973; Collect. Vol. V, p 808.

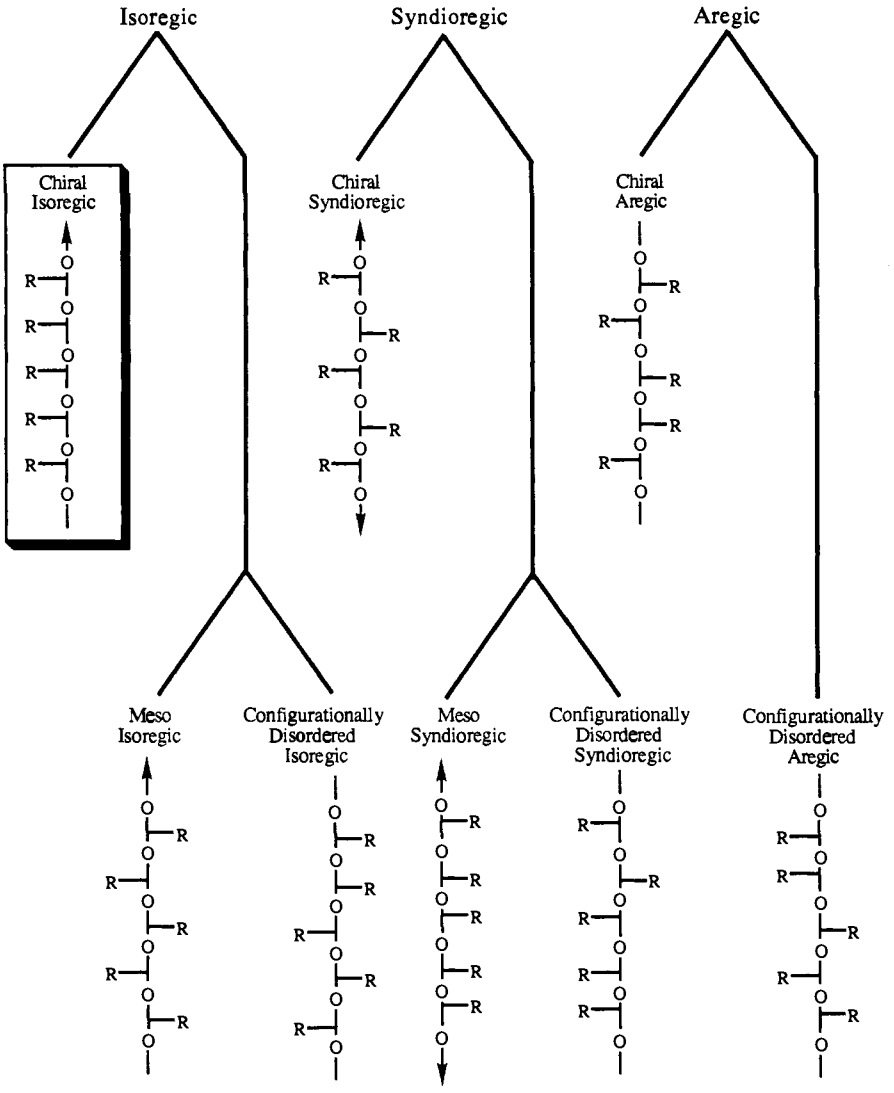

Figure 10. Structural forms of condensation macromolecules including both stereochemical and regiochemical order.

into two well resolved singlets of equal intensity, each corresponding to one of the diastereomers. The diastereomerically enriched compound gave only a single doublet before decoupling and a lone singlet after decoupling. Since this resonance occurs in an uncongested region of the spectrum, the decoupled formyl proton was useful to measure de. Following alkylation, hydrazone-to-nitrile functional group interconversion was performed by methodology developed previously in our laboratory.[13] Excellent yields of racemic nitriles (±)-**4** were obtained from the corresponding DMHs and when these conditions were used for hydrazone (*S*,*S*)-**13a** an 80% yield of nitrile **4a** was obtained with enantiomeric purity around 90%.

The remainder of the synthesis of monomers **5** and the corresponding polymers **2** and **3** is shown in Scheme I. Following hydrazone elimination, deprotection was accomplished in two steps. First, nitriles **4** were desilylated with *n*-tetrabutylammonium fluoride (TBAF) at −78 °C in THF. Complete deprotection required only 30 min even at this temperature. Without further purification, the resulting oily phenol was exposed to a solution of trifluoroacetic acid (TFA) in methylene chloride at room temperature for 30 min. At the end of this time, solvent removal gave crude **5** as a crystalline white solid. A single recrystallization left analytically pure hydroxyacid monomers in 56–66% yield for the two-step deprotection sequence. The monomers were then subjected to the carbodiimide polymerization conditions previously established to give target polymers **2** and **3**. In all cases, good yields of high molecular weight polyesters (dp > 50) were obtained. Two successive precipitations left analytically pure samples as indicated by elemental analysis.

Measurement of ee values by isotope labeling began with the synthesis of the deuteriated nitrile (±)-**4a**-d_3 as shown in Scheme II. Racemic nitrile (±)-**4a** was subjected to a solution of dry Me_2SO-d_6 containing 3 equiv of NaH. After stirring for 2 h at room temperature, the trideuterated phenol, (±)-**6a**, was isolated and purified by preparative TLC. As shown in Scheme II, desilylation was found to accompany proton–deuterium exchange under these conditions. Without further characterization, the phenol was resilylated under standard conditions to obtain deuterium labeled (±)-**4a**-d_3 in 31% overall yield for the two steps. The labeled nitrile, (±)-**4a**-d_3, was then subjected to the two-step deprotection sequence, and each intermediate was fully characterized for dueterium content. These results are summarized in Scheme III. Fluoride ion in THF is known to be somewhat basic,[25] and it was for this reason that desilylation was conducted at −78 °C. The labeled phenol obtained after desilylation, (±)-**6a**-d_3, was then subjected to TFA in methylene chloride in order to remove the *tert*-butyl group.

Synthesis of Model Compounds. The racemic system (±)-**7** was synthesized as shown in Scheme IV. The protected monomer (±)-**4a** was desilylated under standard conditions and immediately acylated with 4-propylbenzoyl chloride to yield (±)-**15**. After purification by column chromatography, the *tert*-butyl group was removed by brief exposure to TFA in methylene chloride and the resulting acid acylated with 4-propylphenol. Following careful purification with silica gel chromatography racemic compound (±)-**7** was obtained in 66% overall yield from (±)-**4a**. Satisfactory ^1H and ^{13}C NMR spectra as well as elemental analysis data were obtained on this compound.

The synthesis of enantiomerically enriched (*S*)-**7** is outlined in Scheme V. Hydrazone (*S*,*S*)-**13a** was desilylated and acylated with 4-(*n*-propyl)-benzoyl chloride to give (*S*,*S*)-**16** in 77% yield. Following purification by column chromatography, the *tert*-butyl protecting group was removed under standard conditions, and the resulting acid was acylated with 4-propylphenol to give (*S*,*S*)-**17** in 75%. At this point ^1H NMR analysis of the decoupled imine proton revealed that no loss in diaste-

(25) Hayami, J.; Ono, N.; Kaji, A. *Tetrahedron Lett.* **1968**, 1385.

reomeric excess had occurred during these synthetic transformations. The SAMP hydrazone was then alkylated with ethyl iodide and subjected to basic elimination with DBN at -78 °C. The conversion of hydrazone (*S,S*)-**17** to nitrile (*S*)-**7** took place in only fair yield, and no attempt was made to improve this reaction. The overall yield of (*S*)-**7** from (*S,S*)-**13a** was 25%. Although no direct measure of ee was made on (*S*)-**7**, it is presumed to be in the range of 70-85% based on results obtained with monomer (*S*)-**4**. Following silica gel chromatography (*S*)-**7** was obtained in analytically pure state and had identical spectral characteristics to its racemate.

Physical Methods of Characterization. Differential scanning calorimetry (DSC) experiments were conducted with a Perkin Elmer DSC 4 differential scanning calorimeter. Typically, heating and cooling rates of 10 °C min^{-1} were employed. Samples for DSC experiments (2-7 mg) were prepared in hermetically sealed aluminum pans. Microscopic observations were made on a Leitz Laborlux 12 pol polarizing microscope coupled to a Leitz hot stage, controlled by a Research, Inc. thermocontroller. Samples were prepared on clean glass surfaces by melting a small particle of the material on the surface at an appropriate temperature. A second glass cover slip was placed on top of the droplet, and the sample was flattened into a thin film.

Acknowledgment. This work was supported by a grant from the Department of Energy, DE AC02 76ER01198, obtained through the Materials Research Laboratory at the University of Illinois. Support for J.S.M. from AT&T Bell Laboratories through a graduate fellowship is also gratefully acknowledged.

Appendix

Figure 9 shows a scheme for deducing the structures of condensation macromolecules at the level of regiochemical order. Chain segments are represented as their Fisher projections where individual monomer units are assembled with a generic linking group symbolized as "-O-". The detailed structure of the linking group is not important for the following discussion. Beginning with a highly substituted, highly symmetric chain, removal of substituents in an orderly fashion will uncover the various levels of macromolecular structure. Removing a pair of substituents from each monomer unit such that each pair is removed from *equivalent positions in adjacent monomers* leaves the *isoregic* backbone. This structure is characterized by its polar translational symmetry. Similarly, removing a pair of substituents from each monomer unit such that each pair is removed from *nonequivalent positions in adjacent monomers* leaves the *syndioregic* backbone. This structure is characterized by its apolar translational symmetry with a periodicity of two monomer units. The *aregic* backbone is obtained by randomly removing pairs of substituents from either equivalent or nonequivalent positions in adjacent monomer units. Chains of this type are not characterized by a single structure but instead by a set of possible constitutional isomers. The aregic backbone thus belongs to the family of chemically disordered polymers.

Figure 10 shows a scheme for deducing the chiral forms of condensation macromolecules. Using Figure 9 as a starting point, stereogenic elements can be introduced by further removal of the remaining substituents on each chain. It can be seen that each of the regiochemical structures can exist in configurationally ordered (top row, Figure 10) as well as configurationally disordered forms (bottom row, Figure 10). Looking first at the disordered forms, it is interesting to note that it is possible to have complete stereochemical and regiochemical order and still have an achiral backbone. The *meso isoregic* and the *meso syndioregic* structures are such examples. The meso isoregic backbone contains a glide-reflection axis along the chain direction, while the meso syndioregic possesses mirror planes perpendicular to the backbone. The configurationally disordered forms of the isoregic and syndioregic backbones as well as the configurationally disordered aregic backbone are systems best described as a set of possible diastereomeric isomers.

Supplementary Material Available: Synthetic procedures for various intermediates and corresponding characterization as well as general information on spectroscopic and chromatographic procedures (42 pages). Ordering information is given on any current masthead page.

Claisen Rearrangement of Allyl Phenyl Ether. 1-^{14}C and β-^{14}C Kinetic Isotope Effects. A Clearer View of the Transition Structure

Lidia Kupczyk-Subotkowska,[1] Witold Subotkowski,[1] William H. Saunders, Jr.,*[,2] and Henry J. Shine*[,1]

Contribution from the Department of Chemistry and Biochemistry, Texas Tech University, Lubbock, Texas 79409, and Department of Chemistry, University of Rochester, River Station, Rochester, New York 14627. *Received October 28, 1991*

Abstract: The kinetic isotope effects, $k^{12}C/k^{14}C$, for the rearrangements of allyl [1-^{14}C]phenyl ether and [β-^{14}C]allyl phenyl ether have been measured: 1.0119 ± 0.0009 and 1.0148 ± 0.0005, respectively. These results, along with those reported earlier for ^{18}O, 2-^{14}C, α-^{14}C, and γ-^{14}C, represent the first complete kinetic isotope effect (KIE) description of a pericyclic system. Modeling calculations have been applied to the heavy-atom KIE and the previously reported deuterium KIE to define the transition structure of the rearrangement more explicitly. The calculations confirm our earlier description that the C_α-O bond is 50-60% broken while the C_γ-C_{ortho} bond is 10-20% formed and now provide significantly more insight to the dynamics of the rearrangement. Coupling between the phenoxy and allyl fragments is stronger, and within the fragments is weaker, than previously supposed.

Introduction

Recently, we reported kinetic isotope effects (KIE) for the four atoms that are directly involved in bond breaking and bond forming in the thermal rearrangement of allyl phenyl ether.[3] That is, we measured the ^{18}O and α-^{14}C KIE of bond breaking and the *ortho*-^{14}C and γ-^{14}C of bond forming. The results were combined with α- and γ-deuterium KIE that had been reported earlier by McMichael and Korver[4] to characterize the transition structure

(1) Texas Tech University.
(2) University of Rochester.

(3) Kupczyk-Subotkowska, L.; Saunders, W. H., Jr.; Shine, H. J. *J. Am. Chem. Soc.* **1988**, *110*, 7153.

0002-7863/92/1514-3441$03.00/0 © 1992 American Chemical Society